Direct Imaging of Loaded Metal−Organic Framework Materials (Metal@MOF-5)

Stuart Turner,*[,†] Oleg I. Lebedev,[†] Felicitas Schröder,[‡] Daniel Esken,[‡] Roland A. Fischer,[‡] and Gustaaf Van Tendeloo[†]

EMAT, University of Antwerp, Groenenborgerlaan 171, B-2020 Antwerp, Belgium, and Anorganische Chemie II—Organometallics and Materials, Ruhr-Universität Bochum, Universitätsstrasse 150, D-44780, Germany

Received April 30, 2008. Revised Manuscript Received July 1, 2008

We illustrate the potential of advanced transmission electron microscopy for the characterization of a new class of soft porous materials: metal@$Zn_4O(bdc)_3$ (metal@MOF-5; bdc = 1,4-benzenedicarboxylate). By combining several electron microscopy techniques (transmission electron microscopy (TEM), high-resolution transmission electron microscopy (HRTEM), electron diffraction (ED), high-angle annular dark-field scanning transmission electron microscopy (HAADF-STEM), and electron tomography) and by carefully reducing the electron dose to avoid beam damage, it is possible to simultaneously characterize the MOF-5 framework material and the loaded metal nanoparticles. We also demonstrate that electron tomography can be used to accurately determine the position and distribution of the particles within the MOF-5 framework. To demonstrate the implementation of these microscopy techniques and what kind of results can be expected, measurements on gas-phase-loaded metal−organic framework materials Ru@MOF-5 and Pd@MOF-5 are presented.

Introduction

In recent years, metal−organic frameworks (MOFs) and other so-called soft materials have received much attention due to their high specific surface area and pore volume.[1−3] This new class of materials shows high promise in gas storage and separation applications as well as in catalysis, gas-sensing, and photovoltaics.[4−7] An important material within this group is $Zn_4O(bdc)_3$ (MOF-5; bdc = 1,4-benzenedicarboxylate), a highly porous material consisting of $\{Zn_4O\}$ building blocks linked together by terephtalate bridges to form a cubic network.[4] In the past, MOF-5 crystals have been loaded with catalytically active material such as palladium, gold, copper, and ruthenium leading to an increased catalytic activity in olefin hydrogenolysis and methanol synthesis.[8,9] Recently, these metal@MOF-5 materials have been produced by gas-phase loading of metal-carrying precursors into the MOF-5 framework.[10] This loading procedure is known to yield a MOF-5 framework loaded with catalytically active nanoparticles in the range of 1−3 nm.[10] To be able to fine-tune the loading procedure, a full characterization of these metal@MOF-5 materials is needed, preferably by one or few techniques. Local knowledge of the state of the MOF-5 framework after loading is needed, as materials like MOF-5 are known to be chemically labile and the loading procedure may affect the framework structure. Along with the state of the MOF-5 framework, information about the size, chemical composition, structure, and distribution of the nanoparticles within the MOF-5 framework is crucial for the design of these materials.

In the present contribution we show that, by minimizing the electron dose to avoid beam damage,[11,12] advanced transmission electron microscopy (TEM) is well-suited to characterize metal@MOF-5 materials on a local scale, as previously demonstrated for other soft porous materials.[11,12] As not all chemical, structural, and spatial information can be provided by one electron microscopy technique; a combination of techniques will be used. Unlike X-ray diffraction (XRD), bright-field TEM and electron diffraction (ED) can provide *local* structural information on the MOF-5 crystals. High-resolution TEM (HRTEM) can directly image the metal particles within the frameworks. Chemical information can be given by high-angle annular dark-field

* Corresponding author. E-mail: Stuart.turner@ua.ac.be.
† University of Antwerp.
‡ Ruhr-Universität Bochum.

(1) Kitagawa, S.; Uemura, K. *Chem. Soc. Rev.* **2005**, *34*, 109–119.
(2) Férey, G.; Mellot-Draznieks, C.; Serre, C.; Millange, F. *Acc. Chem. Res.* **2005**, *38*, 217–225.
(3) Férey, G. *Chem. Soc. Rev.* **2008**, *37*, 191–214.
(4) Li, H.; Eddaoudi, M.; O'Keeffe, M.; Yaghi, M. *Nature* **1999**, *402*, 276–279.
(5) Kitagawa, S.; Kitaura, R.; Noro, S. *Angew. Chem., Int. Ed.* **2004**, *43*, 2334–2375.
(6) Yaghi, O. M.; O'Keeffe, M.; Ockwig, N. W.; Chae, H. K.; Eddaoudi, M.; Kim, J. *Nature* **2003**, *423*, 705–714.
(7) Férey, G.; Mellot-Draznieks, C.; Serre, C.; Millange, F.; Dutour, J.; Surblé, S.; Margiolaki, I. *Science* **2005**, *309*, 2040–2042.
(8) Hermes, S.; Schroeter, M.-K.; Schmid, R.; Khodeir, L.; Muhler, M.; Tissler, A.; Fischer, R. W.; Fischer, R. A. *Angew. Chem., Int. Ed.* **2005**, *44*, 6237–6241.
(9) Sabo, M.; Henschel, A.; Froede, H.; Klemm, E.; Kaskel, S. *J. Mater. Chem.* **2007**, *17*, 3827–3832.
(10) Schröder, F.; Esken, D.; Cokoja, M.; van den Berg, M. W. E.; Lebedev, O. I.; Van Tendeloo, G.; Walaszek, B.; Buntkowsky, G.; Limbach, H.-H.; Chaudret, B.; Fischer, R. A. *J. Am. Chem. Soc.* **2008**, *130* (19), 6119–6130.
(11) Lebedev, O. I.; Millange, F.; Serre, C.; Van Tendeloo, G.; Férey, G. *Chem. Mater.* **2005**, *17*, 6525–6527.
(12) Kremer, S. P. B.; Kirschhock, C. E. A.; Aerts, A.; Villani, K.; Martens, J. A.; Lebedev, O. I.; Van Tendeloo, G. *Adv. Mater.* **2003**, *15*, 1705–1707.

10.1021/cm801165s CCC: $40.75
Published on Web 08/07/2008

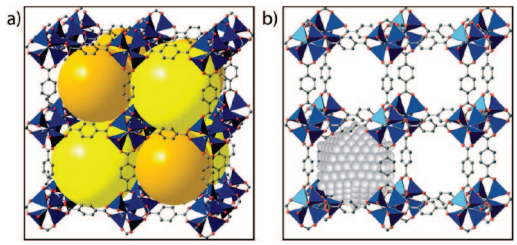

Figure 1. MOF-5 and metal@MOF-5 structure: (a) Unit cell of MOF-5. (b) Cut-out model of metal@MOF-5. The model only displays one possible way of embedding an ideal, icosahedral, three-shell, hexagonal close-packed (hcp) ruthenium cluster of 1.5 nm in an MOF-5 cavity, not the real distribution of metal nanoparticles over the MOF-5 matrix.

Table 1. Chemical Composition and Porosity of the Metal@MOF-5 Materials

	chemical composition [wt %]			porosity
sample	metal loading	C	H	$S_{Langmuir}$ [m^2/g]
Ru@MOF-5	30.6	25.5	1.06	860
Pd@MOF-5	27.7	41.41	3.634	1091

scanning transmission electron microscopy (HAADF-STEM) imaging. Electron tomography provides spatial information, i.e., the uniform or random distribution of the particles throughout the MOF matrix. With the introduction of this technique, determination of the exact position and distribution of particles within a framework is possible.

Materials and Methods

Material Structure and Preparation. The MOF-5 metal−organic framework structure is made up of ZnO_4 tetrahedra linked by 1,4-benzenedicarboxylate linkers to form a cubic lattice (space group $Fm\bar{3}m$, lattice parameter $a = 25.909$ Å) (Figure 1a). To load the MOF-5 frameworks with metal particles, a gas-phase loading procedure has been adopted.[10] In the present work, two types of gas-phase-loaded metal@MOF-5 materials have been studied: ruthenium-loaded MOF-5 (Ru@MOF-5) and palladium-loaded MOF-5 (Pd@MOF-5). Both samples were synthesized using porous $Zn_4O(bdc)_3$. The MOF-5 framework was loaded with a [Ru(cod)(cot)] (cod = 1,5-cyclooctadiene; cot = 1,3,5-cycloocatriene) or palladium precursor [(η^5-C_5H_5)Pd(η^3-C_3H_5)] in vacuo to form an intermediate material: precursor@MOF-5.[8,10] Subsequent hydrogenolysis of [Ru(cod)(cot)]@MOF-5 or photolysis of [(η^5-C_5H_5)Pd(η^3-C_3H_5)]@MOF-5 yielded metallic nanoparticles within the pores of the original MOF-5 framework.[8,10] The structure of metal@MOF-5 materials is shown in Figure 1b. The particles have approximately the same size as the diameter of the framework pores (1.5 nm (larger pore) and 1.1 nm). The gas-phase loading procedure used for the present study can lead to a maximal loading of 30 wt % metallic particles.[8]

Elemental analysis was performed by the Analytical Laboratory of the Catalysis Research Center of Süd Chemie AG, Heufeld, Germany (Ru@MOF-5) and in the department of Analytical Chemistry of the Ruhr-University Bochum (Pd@MOF-5). The measurements were performed by standard protocols employing inductively coupled plasma atom emission spectroscopy (ICP-AES) (Ru@MOF-5) or an atomic absorption spectroscopy (AAS) apparatus by Vario of type 6 (1998) (Pd@MOF-5); C and H analyses were carried out using a Vario CHNSO EL (1998) instrument. Elemental composition of the samples is given in Table 1.

TEM Sample Preparation. For TEM investigation the metal@MOF-5 samples were prepared by suspending the powder materials in dry toluene and subsequently placing a few drops of the suspension on carbon-coated Cu grids and drying overnight. All preparation was performed in a glovebox under an inert gas stream. During transportation the samples were stored in a Schlenk flask filled with argon.

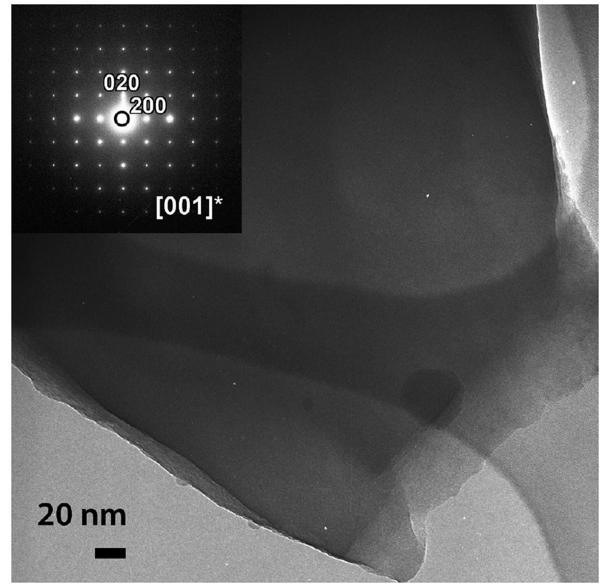

Figure 2. Empty MOF-5 framework: bright-field TEM image of an empty MOF-5 crystal. The pores of the framework are not observable by TEM. The inset diffraction pattern evidences the cubic structure of MOF-5 and confirms that the MOF-5 crystal structure is still (largely) intact.

(HR)TEM, ED, HAADF-STEM, and Electron Tomography. Bright-field TEM and ED experiments were performed on a Philips CM20 microscope, operated at 200 kV. High-resolution TEM was performed on a JEOL 4000EX, operated at 400 kV and having a 1.7 Å point resolution. Tomography and HAADF-STEM experiments were performed on a JEOL 3000F TEM−STEM microscope, operated at 300 kV and equipped with a −70° to +70° tomography tilt stage and holder. Images for tomographic reconstruction were taken using a 2° interval, over the largest possible angle (preferably 140°). A reference image taken at 0° tilt was taken before and after image acquisition, to ensure no changes in the sample structure due to beam damage occurred during acquisition. Tomographic reconstruction was performed using the MATLAB tomography toolbox. HAADF-STEM images were taken at a nominal spot size of 0.5 nm. The HAADF inner collection semiangle was 35 mrad.

For all techniques low-intensity beam conditions (lowest possible magnification, low beam intensity, and long exposure times) were used as much as possible to minimize the electron dose and possible beam damage of the metal−organic framework. The images for the tomographic acquisition were taken in bright-field TEM instead of HAADF-STEM. Bright-field TEM had to be used for the tomography images (although unwanted diffraction contrast inevitably occurs with this technique), as prolonged STEM illumination damaged the samples.

Results

MOF-5 Framework. Within a single batch of metal@MOF-5 material, crystals with varying degrees of particle filling could be found. This is due to the high mobility of the precursor molecules within the MOF-5 framework. Upon decomposition (hydrogenolysis for Ru@MOF-5 and photolysis for Pd@MOF-5) the resulting "liberated" metal atoms from different molecules will fuse to nanoparticles leaving some cavities completely empty.[10] Figure 2 shows a typical

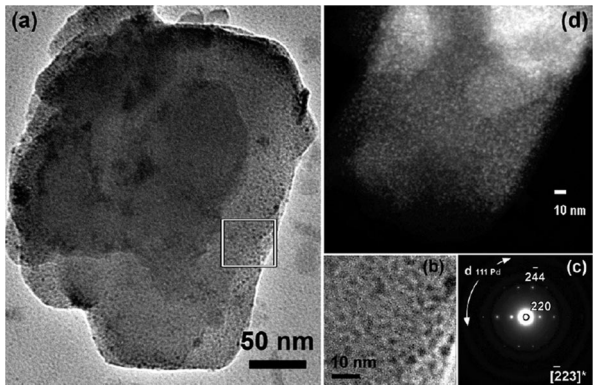

Figure 3. Pd@MOF-5: (a) Bright-field TEM image showing the Pd-loaded framework; the crystal is faceted, indicating that the framework is still intact after loading. (b) Enlarged image of the region indicated in (a); the particles have sizes ranging from 1 to 3 nm. (c) Diffraction pattern taken from a cubic Pd@MOF-5 crystal in the [−223] zone axis. A weak ring corresponding to the 111 planes of cubic Pd is also visible. (d) HAADF image of the Pd@MOF-5 material showing the Pd particles as white spots.

low-magnification bright-field TEM image of an empty MOF-5 crystal. In most cases the MOF-5 crystals are faceted, indicative of an ordered framework structure. The ED pattern of the MOF-5 crystal in Figure 2 shows well-defined reflections corresponding to the [001] zone axis orientation of the cubic framework structure. This diffraction information indicates that the framework is still (largely) intact and that it can therefore withstand the electron beam at low dose. HRTEM to directly resolve the porous cavities of the framework failed, although the cavities lie well within the resolution of the instrument. This fact is clearly attributed to electron beam degradation of the MOF-5 pores.[10]

Metal@MOF-5. A typical Pd@MOF-5-loaded framework is shown in Figure 3. The bright-field TEM image in Figure 3a shows that the MOF crystal is partially faceted, indicating—as with the empty MOF matrix—that there is no large-scale collapse of the metal−organic framework. Figure 3b is an enlarged image of the area indicated in Figure 3a; 1−3 nm sized particles can be clearly imaged within the framework. The pore diameters of MOF-5 are 1.5 (larger pores) and 1.1 nm. Metal particles in the MOF-5 with a larger diameter are most probably located in a locally distorted MOF-5 environment or at the surface. Similar observations have been made for metal nanoparticles in zeolitic materials.[13] The diffraction pattern (Figure 3c) shows that the cubic MOF structure is still intact; the crystal is imaged along the [−223] zone axis. Together with the diffraction spots attributed to the MOF-5 framework, a faint ring is visible in the diffraction pattern. This ring at 2.25 Å is typical for the (111) spacing of cubic palladium. The ED pattern therefore not only shows that the MOF framework is still intact but also that the embedded 1−3 nm particles are crystalline and have the cubic Pd structure ($Fm\bar{3}m$, space group 225 with lattice parameter $a = 3.9$ Å). An HAADF-STEM image of a similar Pd-loaded crystal is shown in Figure 3d. The contrast in this type of image depends on both the thickness of the sample and the atomic number Z and, therefore, contains chemical information. The heavier Pd nanoparticles

(13) Kampers, F. W. H.; Engelein, C. W. R.; van Hoff, J. H. C.; Koningsberger, D. C. *J. Phys. Chem.* **1990**, *94*, 8574–8578.

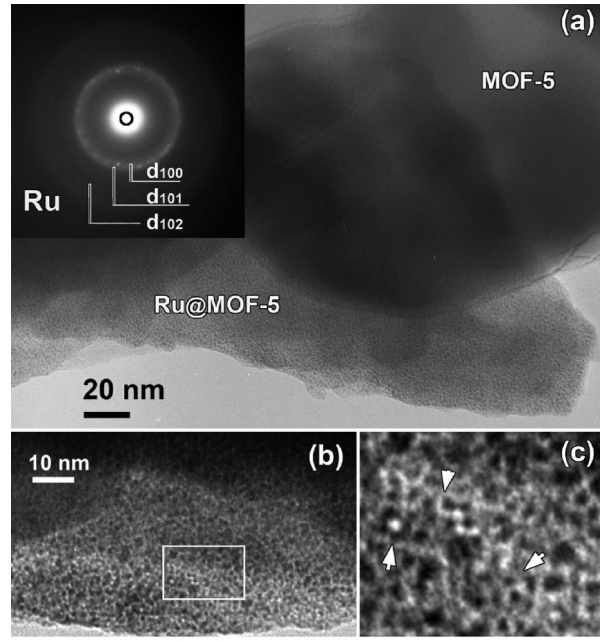

Figure 4. Ru@MOF-5: (a) Bright-field TEM image of an empty MOF-5 crystal (right top) and a ruthenium-loaded framework (bottom); the inset diffraction pattern, taken from the loaded crystal, shows rings typical of the hexagonal crystal structure of the loaded Ru particles. (b) Enlarged image; the matrix is densely loaded with particles. (c) Enlarged image of the region indicated in (b). The arrows indicate regions where local ordering of the particles can be seen.

appear as bright white dots within the MOF-5 framework. The particles appear to be closely packed, in agreement with previous measurements of the average particle loading of 30 wt %.[8]

To investigate the impact of a different precursor decomposition procedure on the metal nanoparticle distribution, a loaded Ru@MOF-5 matrix obtained by hydrogenolysis of [Ru(cod)(cot)]@MOF-5 was also examined. In Figure 4a, two MOF-5 crystals with varying degrees of particle filling are shown. The crystal indicated as MOF-5 is almost empty; the crystal labeled Ru@MOF-5 is densely packed with particles ranging from 1 to 3 nm in size. The inset diffraction pattern is taken from this crystal and evidences that also the Ru particles are crystalline and have a hexagonal structure ($P6_3/mmc$, space group 194 with lattice parameters $a = b =$ 2.7 Å and $c = 4.3$ Å). In Figure 4b an enlarged image of Figure 4a is presented. The closely packed particles appear in many cases to establish a degree of ordering. This short-range ordering is visible in Figure 4c (indicated by arrows) and stretches only for 4−5 particles. These results indicate that the large degree of particle loading obtained for Pd@MOF-5 can also be obtained with Ru.

In Figure 5 HRTEM images of the same Ru@MOF-5 system are obtained. By focusing the electron beam in HRTEM the MOF structure is destroyed, but the particles remain intact. In Figure 5a, particles with a size of 1−3 nm are imaged. The particles are monocrystalline ruthenium, with lattice fringes in agreement with the hexagonal structure. In Figure 5b, a system with only smaller particles (<2 nm) is imaged. Less lattice fringes are visible, as charging of the samples occurs due to the size of the particles, distorting the HRTEM image. Once again the system appears to be

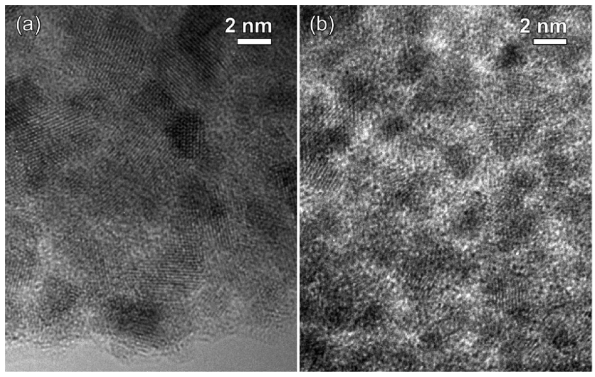

Figure 5. Ru@MOF-5: typical high-resolution image of a metal@MOF-5-type material. (a) Size and shape of the 1−3 nm loaded nanoparticles is clearly visible. (b) Material containing only smaller particles (1−2 nm). Charging occurs in these samples, making HRTEM imaging difficult.

closely packed with particles. Because of the beam damage and because of the two-dimensional aspect of the image, it is not possible to resolve the spatial position of the particles within the MOF-5 framework. On the other hand, to optimize the metal@MOF-5 material synthesis and loading procedures, knowledge of the exact positioning of the metal nanoparticles within the MOF-5 framework is needed. This information can be provided by electron tomography.

The potential of electron tomography for metal@MOF-5 characterization and particle positioning within the MOF-5 framework is tested by performing tomography experiments on samples with varying degrees of particle penetration into the MOF-5 matrix, namely, the Ru@MOF-5 and Pd@MOF-5 samples. It can be expected that the difference in synthesis of the Pd@MOF-5 and Ru@MOF-5 samples leads to a difference in particle penetration or distribution. Pd@MOF-5 was synthesized under mild conditions via photolysis at room temperature. Ru@MOF-5 was obtained via hydrogenolysis at elevated temperature and pressure which will have some impact on the particle distribution throughout the MOF network. Bright-field TEM tomography is used to minimize the electron beam damage during the long acquisition needed for the tomographic reconstruction.

In Figure 6, a Pd@MOF-5 crystal with a high metal particle density/penetration is imaged. The bright-field TEM image (Figure 6a) shows particles closely packed together within the MOF-5 framework. The inset shows that the particles have sizes ranging from 1 to 5 nm, although structures larger than 3 nm appear to be agglomerates. These agglomerates are mostly positioned at the MOF-5 surface. Figure 6b is the tomographic reconstruction of the particles within the MOF-5 framework. As was clear from the bright-field TEM image, the particles are densely packed inside the MOF-5 matrix. Two slices through the tomographically reconstructed volume are presented in Figure 6, parts c and d. Both slices show large amounts of particles spread within the bulk of the framework. The particles within the framework have typical sizes ranging from 1 to 3 nm. Parts c and d of Figure 6 also show that the larger particles/agglomerates are mostly positioned at the surface of the MOF-5 crystal (indicated by arrows in Figure 6, parts c and d).

In contrast, a Ru@MOF-5 sample with low particle penetration is imaged and reconstructed in Figure 7. The

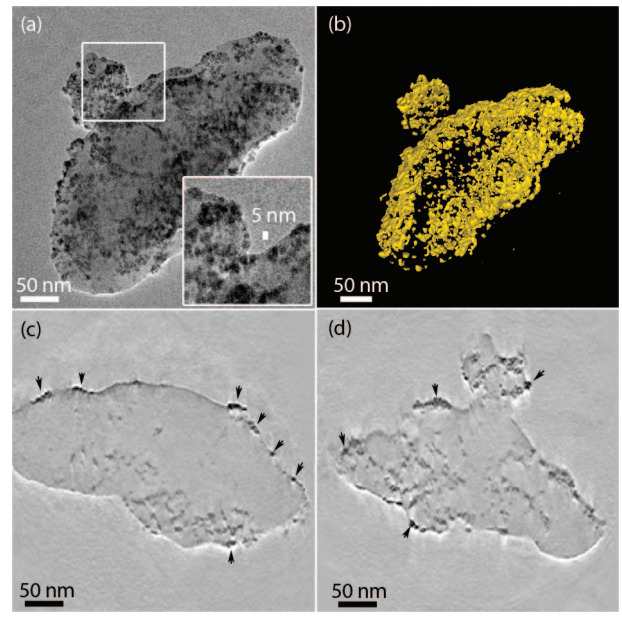

Figure 6. Pd@MOF-5—fully loaded: (a) Bright-field TEM image of a Pd-loaded MOF; the inset shows particles from 1 to 5 nm in diameter are present; some particles appear to have agglomerated. (b) Tomographically reconstructed Pd particles (matrix not imaged). (c and d) Slices through the tomographically reconstructed volume; the metallic particles are imbedded inside the MOF-5 matrix. The particles that are at the surface of the crystal are larger or have formed agglomerates.

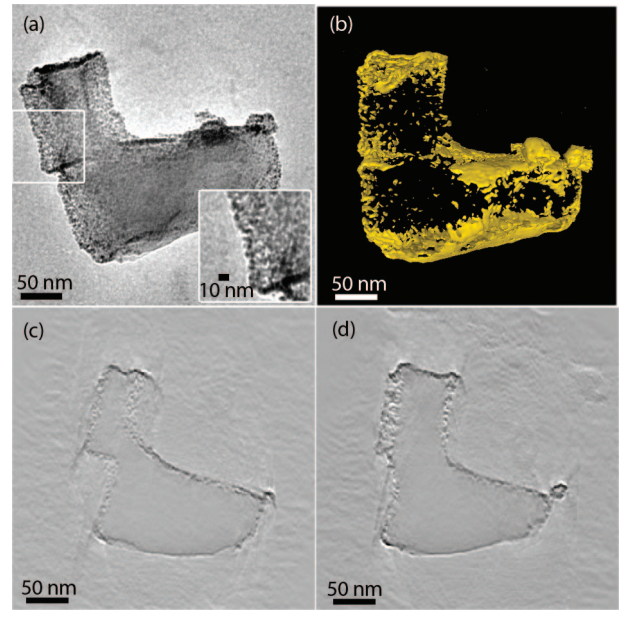

Figure 7. Ru@MOF-5—not fully loaded: (a) Bright-field TEM image of a Ru-loaded MOF; the inset shows particles from 1 to 5 nm in diameter are present; the matrix appears to be densely packed. (b) Tomographically reconstructed Pd particles (matrix not imaged); some overlapping of the particles is present due to diffraction contrast. (c and d) slices through the tomographically reconstructed volume; the metallic particles are not imbedded inside the MOF-5 matrix. All particles are positioned at the surface of the matrix or close to the surface (up to approximately 20 nm deep).

bright-field TEM image of Figure 7a gives the impression that the distribution of the particles within the MOF-5 framework is homogeneous and densely packed, with particles once again in the 1−5 nm size range. The three-dimensional (3D) tomographic reconstruction of the particles within the MOF-5 framework in Figure 7b, however, shows a complete different picture. It is clear that the particles are

not spread throughout the framework. The slices through the tomographically reconstructed volume, parts c and d of Figure 7, clearly show that the particles are in fact located at or close to the surface of the MOF-5 structure and have a maximum penetration depth of 20 nm. This illustrates that one has to be very careful in interpreting projected images when it comes to 3D distributions. The positioning of the particles toward the surface of these metal@MOF-5-type materials could certainly not be predicted from the bright-field image alone.

Discussion

Sample Stability to Beam Damage. It is clear from the data presented that advanced TEM is a promising technique for the characterization of loaded metal@MOF-5 materials. All information obtained using electron microscopy must, however, be carefully interpreted as MOF materials are notoriously easy to damage under an intense electron beam. In the present work, the metal@MOF-5 materials appear to remain structurally stable under the beam, even during prolonged experiments like a tomographic acquisition. This apparent stability is evidenced by the diffraction experiments performed on empty (native) MOF-5 cubic crystals (Figure 2), indicating that the structure of the framework remains intact under a low-intensity electron beam. It should, however, be mentioned that diffraction patterns cannot be acquired for all MOF-5 sample crystals. In most of the (bright-field) TEM results the MOF-5 crystals have a faceted shape showing straight crystal faces. This typical faceted shape is a visualization of the MOF-5 crystal structure and a second indication of the stability of the crystals under the electron beam. This stability is only maintained because of the low electron dose used during the experiments (lowest possible magnification, low beam intensity, and long exposure times).

However, a limited amount of degradation to the MOF-5 crystals under the beam is unavoidable. The fact that no pore structure can be observed in HRTEM in empty MOF-5 crystals is probably the result of a local degradation of the crystal structure under the electron beam. The TEM experiments should therefore be carried out and interpreted with great care and, where possible, backed up by diffraction evidence.

HAADF-STEM images need to be taken with very short exposure times, as prolonged probe scanning on the samples does cause beam damage and unwanted growth. HAADF-STEM imaging was therefore not used to obtain the tomographic reconstructions.

MOF-5 Framework Loading. In the past, it has been shown the gas-phase loading procedure, used to produce current samples Ru@MOF-5 and Pd@MOF-5, does not damage the already chemically labile MOF-5 framework.[10,14] The results presented in Figure 3, containing diffraction information of the host MOF framework and the loaded particles simultaneously, confirm that the MOF-5 framework can withstand a gas-phase loading procedure. Moreover, the loading procedure and the subsequent presence of the nanoparticles within the pores of the framework may actually enforce the MOF crystals. TEM revealed, however, that the loading of the particles is not always uniform. Some MOF-5 crystals are closely packed with metal particles, whereas others are hardly loaded, or not at all (Figure 4).

In all samples particles with a size ranging from 1 to 3 nm are observed. Larger particles in Figures 6 and 7 are in fact agglomerates, which usually form at the surface of the MOF-5 crystals. The observed particle sizes fit well with the metal@MOF-5 model, which implies that the particles need to be of the order of 1−3 nm in order to be nestled inside the framework pores (15 Å for the larger pores and 11 Å for the smaller pores). Presuming the metal@MOF-5 model is correct, the arrangement of the particles within the framework could be an extra indication of the state of the MOF-5 framework after loading. As the framework consists of cubically arranged pores, it is not surprising that the metal nanoparticles follow this arrangement (as long as the framework remains intact) and that some ordering takes place. Some indication of short-range ordering in the particle position is observed in Figure 4. In the bright-field TEM image the metal particles appear to be arranged in small groups (indicated by arrows in Figure 4c). Arrangements only stretch 4−5 particles, as not all pores of the framework are filled. The local arrangement of the particles in Figure 4 is an indication that, even if the MOF-5 crystals are degraded by the beam, the particles are imbedded within the structured framework of the MOF-5 crystals and that this framework remained highly ordered after loading.

The loaded metal nanoparticles can be imaged using HRTEM. In some cases, however, the sample charges under the electron beam and makes acquisition of clear HRTEM images difficult (imaging at lower magnification does not cause charging problems). Charging mostly occurs in samples with particles smaller than 2 nm (Figure 5b). When larger particles (>2 nm) or surface agglomerates are present (Figure 5a) HRTEM imaging in no longer hindered by sample charging. The lack of this charging effect in the presence of larger particles is probably caused by the presence of some of these larger particles and agglomerates at the surface of the MOF-5 framework. When present, these surface particles conduct the charge away from the sample, whereas when only small (embedded) particles are present, charge can accumulate.

The tomography results show that it is possible to accurately determine the local degree of MOF-crystal filling and to position the metal nanoparticles within the MOF-5 framework. In the present samples Ru@MOF-5 and Pd@MOF-5 tomography easily discerned two cases: a fully loaded MOF-5 framework (Figure 6) and a framework material with a small degree of particle penetration (Figure 7). The slices through the tomographically reconstructed volume show that the small (1−3 nm, not agglomerated) particles are nestled within the metal−organic framework, whereas the larger structures and agglomerates are present only at the surface of the MOF-5 matrix. In the case of Ru@MOF-5, these surface particles probably form during the prolonged hydrogenolysis of the starting material [Ru(cod)(cot)]@MOF-5 to Ru@MOF-5.

(14) Hermes, S.; Schroeder, F.; Amirjalayer, S.; Schmid, R.; Fischer, R. A. *J. Mater. Chem.* **2006**, *16*, 2464–2472.

Due to diffusion limitation of the H_2 gas, particle formation will probably start at the surface of the MOF-5 matrix. The highly mobile (see above) [Ru(cod)(cot)] precursor molecules from the inner core of the MOF-5 matrix will then diffuse to the outer surface of the crystallites as well to form Ru nanoclusters. The formation of these surface agglomerates is not due to beam damage, as the surface agglomerates are already visible on the first image taken for acquisition, and the configuration does not change during acquisition of all images for tomography. The results in Figure 7 show that tomography is an extremely important tool to determine the position of the particles within the MOF-5 framework. The bright-field TEM image of the same sample taken at 0° inclination appears to image a closely packed, fully filled MOF-5 matrix. Tomography, however, clearly places the particles toward the surface of the crystal, with a maximum penetration depth of 20 nm. It is therefore clear that tomography is needed for a full local characterization. However, great care should be taken not to damage the samples by long exposure to the beam.

Conclusion

We have shown that, by reducing the electron dose to avoid beam damage, TEM is well-suited to locally characterize metal@MOF-5 loaded nanoporous materials. Electron diffraction and conventional bright-field TEM have been used to show that the loading of the MOF-5 frameworks using a gas-phase loading procedure results in a largely intact structure of the MOF-5 crystals. HRTEM and HAADF-STEM have successfully shown that these framework crystals contain varying amounts of monocrystalline, metallic particles embedded within the framework pores with sizes ranging from 1 to 3 nm. Larger particles tend to aggregate at the surface. These results also suggest a local short-range ordering of these nanoparticles, which would be consistent with the fact that they are imbedded within the pores of the cubic MOF-5 framework as foreseen in the metal@MOF-5 model. Electron tomography allowed us to distinguish between fully loaded metal@MOF-5 materials and materials with a limited particle penetration into the MOF-5 matrix. Electron tomography can be used to accurately describe the distribution of the metallic particles embedded within the MOF pores and the degree of agglomeration of the particles at the crystal surface, giving full spatial information on these loaded materials.

Acknowledgment. S.T. kindly acknowledges professor Sara Bals for her help with electron tomography. The authors acknowledge support from the European Union under the Framework 6 program under a contract from an Integrated Infrastructure Initiative (Reference 026019 ESTEEM). This work was also founded within the Research Centre 558 “Metal-Substrate Interactions in Heterogeneous Catalysis” by the German Research Foundation (DFG). F.S. is grateful for a scholarship by the German National Academic Foundation and a fellowship by the Research School of the Ruhr-University Bochum.

CM801165S